

Propagation of laser-supported ionization wave in an underdense target

J. Limpouch¹, S. Yu. Gus'kov², V.T. Tikhonchuk³

¹*Czech Technical University in Prague, FNSPE, Brehova 7, 115 19 Praha 1, Czechia*

²*P. N. Lebedev Physical Institute of Russian Academy of Sciences, Moscow 119991, Russia*

³*Centre Lasers Intenses et Applications, Université Bordeaux - CNRS - CEA, Talence 33405, France*

1. INTRODUCTION

The physics of interaction of high intensity laser radiation with low density materials is of major importance for many applications, in particular in inertial confinement fusion. In the indirect drive scheme [1], the laser beams propagate through a gas filled hohlraum before depositing their energy to the walls. In the direct drive scheme, various target designs are considered [2] in order to avoid the initial laser pulse intensity fluctuations to be imprinted on the target surface and further amplified. Smoothing of small scale inhomogeneities by radiation driven ionization wave in foam was verified experimentally [3], however, radiation can lead to an undesirable fuel preheat. It was suggested in Ref. [4] to use underdense foams that could be ionized by the laser pulse itself. Supersonic ionization wave and an efficient smoothing of the transmitted laser beams were demonstrated at LIL laser facility [5].

The physics of laser propagation through low density gas targets was investigated via an analytical model and hydrodynamic simulations [6]. Direct numerical simulations of laser interaction with foams are very complicated because of the foam structure of typically micrometer pore size with solid elements tens of nanometres thick. The ionization front velocity in numerical simulations using a homogeneous medium of the equivalent density and composition is significantly higher compared to the measurements [7, 8]. It is explained by the delay due to the time required for the opaque solid density elements to expand to the density lower than the critical one [9]. In the present paper, we develop a model of a quasi-stationary ionization wave continuously supported by the laser energy deposition that can be applied for homogeneous and porous underdense materials.

2. IONIZATION FRONT IN A HOMOGENEOUS MATERIAL

Plasma heating and laser absorption in the plane geometry are described, as follows

$$\frac{3}{2} n_a \frac{\partial}{\partial t} (Z_{av} T_e) + n_a \chi_{[Z_{av}]^{+1}} \frac{\partial Z_{av}}{\partial t} = \kappa_{ei} I_L = - \frac{\partial I_L}{\partial z} \quad , \quad (1)$$

where we take into account ionization from the charge state $[Z_{av}]$ only, and n_a is the atom (ion) density, T_e is the electron temperature, $Z_{av} = n_e/n_a$ is the mean ion charge, n_e is the

electron density, χ_j is the ionization potential to the j -times ionized ion, I_L is the laser intensity and the coefficient κ_{ei} of the collisional laser absorption is $\kappa_{ei} = \kappa_0 T_e^{-3/2}$.

In fully ionized plasma, analytical solution has been found in Ref. [6]

$$T_e^{3/2} = \frac{3\kappa_0}{2}(z_f - z) \quad I_L^{3/2} = I_0^{3/2} \left(1 - \frac{z_f}{z}\right) \quad V_{f\dot{t}} = \frac{dz_f}{dt} = \frac{2I_0}{3n_e} \left(\frac{3\kappa_0}{2} z_f\right)^{-2/3}, \quad (2)$$

where $I_0(t) = I_L(0, t)$ is the incident laser intensity and $z_f(t)$ is the heat front position. Figure 1a) shows the spatial profile of the plasma temperature and the laser intensity.

When plasma is not fully ionized, ionization front of width Δz_f is formed at the point z_{if} (Fig. 1b). The equations (1) have to be supplemented by the following ionization rate equation

$$\frac{\partial Z_{av}}{\partial t} = Z_{av} n_a S_{[Z_{av}]+1} ([Z_{av}] + 1 - Z_{av}) \Psi \left(\frac{T_e}{[Z_{av}] + 1} \right). \quad (3)$$

The system (1), (3) has been analyzed numerically in Ref. [6]. In our simplified treatment, we approximate $\Psi(x) \approx 0.2H(x-1)$ via Heaviside step function and ionization potential is $\chi_Z \approx \chi_H Z^2$. The ionization rate is expressed $n_a S_Z \approx \nu_{ion} Z_{av}^{-3}$, where $\nu_{ion} \approx 2 \times 10^4 \rho_a / A \text{ ps}^{-1}$ is the ionization frequency. Then the equation (3) takes the simple form (Z_m is the nuclear charge)

$$\frac{\partial Z_{av}}{\partial t} = \frac{\nu_{ion}}{Z_{av}^2} \quad \text{if } (T_e \geq \chi_H Z_{av}^2 \text{ and } Z < Z_m), \quad \text{and} \quad \frac{\partial Z_{av}}{\partial t} = 0 \quad \text{otherwise.} \quad (4)$$

The second term in Eq. (1), representing the ionization energy, is relatively small compared to the first one. Consequently, the first part of (1) can be rewritten

$$\frac{\partial}{\partial t} (Z_{av} \theta) \approx \nu_h Z_{av}^3 \theta^{-3/2} \quad \nu_h \equiv \xi_h I_L \approx 1.6 \times 10^5 I_{14} \lambda_L^2 \rho_a / A \text{ ps}^{-1}, \quad (5)$$

where $\theta = T_e / \chi_H$ is the dimensionless temperature and I_{14} is the laser intensity in 10^{14} W/cm^2 .

At low laser intensities, $I_0 \leq I_B = 3 \nu_{ion} / \xi_h$, the heating rate is smaller than the ionization rate. Then the ionization equilibrium is established in each moment and $Z_{av}^2 = \theta$. When this

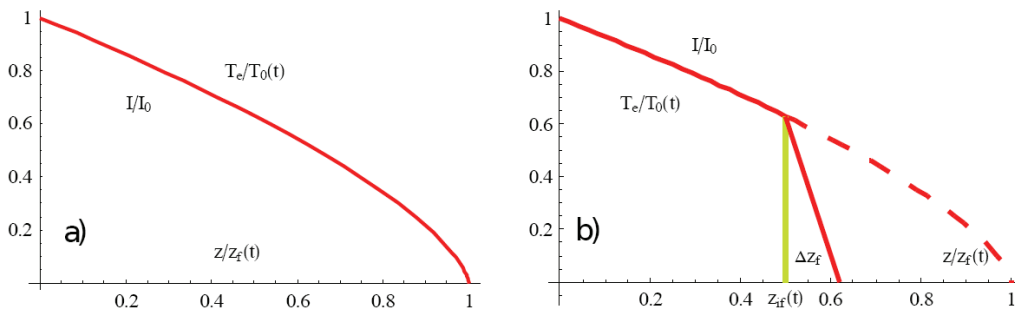


FIG. 1: Spatial distribution of the laser intensity and the electron temperature in the thermal/ionization wave: a) the case of fully ionized plasma; b) the case of non-ionized homogeneous medium. Here, Δz_f is the ionization front width and z_{if} is the point where the ionization is terminated and the ionization front joins the thermal wave.

relation is substituted to the energy conservation, the temperature is increasing linearly with time $\theta = Z_{av}^2 = \int v_h dt \approx v_h t$, until Z_m is reached. On the other hand, at high heating rates $v_h > 3 v_{ion}$, ionization does not catch up with the temperature and plasma is overheated with the mean ion charge Z_{av} less than in the equilibrium, and it is increasing as $Z_{av} = (3 v_{ion} t)^{1/3}$. For the constant laser intensity, the temperature evolves as $\theta \approx v_h^{2/5} (3 v_{ion})^{4/15} t^{2/3}$.

3. IONIZATION FRONT IN AN UNDERDENSE POROUS MATERIAL

Propagation of the ionization wave in an underdense porous material is slowed down in comparison with the case of homogeneous medium of the same density by the process of filling the pore by expanding solid elements. The front advances further only after the density of expanding plasma drops below the critical value. The porous material has a structure, which is a mixture of thin membranes and wires of a solid density ρ_s . It is characterized by the thickness of solid elements, δ_s , which is of the order of tens of nanometres, and the distance between them, δ_0 , which is approximately equal to the pore size. Depending on the fabrication technology, the pore size in the foams made of light elements can vary from several microns to tens or even hundred microns. We are considering here small pore foams with the size δ_0 much smaller than the front thickness and the thickness of the foam layer.

The relation between the size of the structural elements and the pore size depends on their topology, fabrication technology, and the average foam density ρ_a . In general, the thickness $\delta_s \approx \delta_0 (\rho_a / \rho_s)^\alpha$ where $\alpha = 1$ for foil-like structures corresponding to closed pores and $\alpha = 1/2$ for wire-dominated foams with open pores. The detailed analysis of the properties of porous materials shows that the typical size of the structural elements can be characterized by a fractal dimension $\alpha \approx 0.8$ [10].

In our analysis of the homogenization process, we assume that the solid elements are heated almost homogeneously. Knowing the time τ_f needed for the density to decrease from the initial level ρ_s to the critical density ρ_{cr} , one can suppose that the front progresses by one pore distance each time as the element explodes. Consequently, the characteristic velocity of the laser penetration into a porous material can be estimated as $V_p \approx \delta_0 / \tau_f$. The ionization rate at the solid density is higher than the heating rate. Isothermal rarefaction wave propagates to the centre of solid element, and then the maximum density decreases due to the foil expansion. The foil becomes transparent, when the maximum density is equal to the critical density n_{cr} at the time $\tau_f \approx \delta_s Z_m n_s / n_{cr} c_s$, where c_s is the ion sound velocity. Using energy

conservation, the ion sound velocity c_s is expressed via the laser intensity I_L , and the propagation velocity of the ionization front is evaluated, as follows

$$V_p \approx \frac{n_{cr}^{2/3} I_L^{1/3}}{(4m_i Z_m^2)^{1/3} n_a^\alpha n_s^{1-\alpha}} \approx 9.7 \times 10^4 \frac{A^{2/3} I_{14}^{1/3}}{Z_m^{2/3} \lambda_L^{4/3} \rho_a^\alpha \rho_s^{1-\alpha}} \text{ cm/s} . \quad (6)$$

In the recent experiment [5], a polymer foam with a chemical composition $C_{15}H_{20}O_6$, the average mass density $\rho_a = 6 \text{ mg/cm}^3$, thickness of 500 - 900 μm and the pore size of the order of 1-2 μm was employed for the studies of the laser beam smoothing. The average laser intensity was $4 \times 10^{14} \text{ W/cm}^2$ ($\lambda_L = 351 \text{ nm}$) in a 3 ns square pulse. The ionization front propagation velocity was supersonic and was decreasing with time from 600 to 400 km/s. For such foam, the effective charge and mass numbers are $Z_m = 3.85$ and $A = 7.22$. Then, Eq. (6) gives the front velocity $V_p \approx 570 \text{ km/s}$ for $\alpha = 0.8$ in a good agreement with the experiment. On the contrary, a strongly overestimated front velocity of 1580 km/s is obtained for $\alpha = 1$.

4. CONCLUSIONS

A one-dimensional model of the propagation of the laser-supported ionization wave in under-critical gases and foams is developed. The upstream material is supposed to be cold and non-ionized. The ionization takes place in a narrow zone in the front and the downstream laser intensity profile is defined by the balance between the incident laser flux and electron heating. The ionization wave in foam targets is slowed down due to the fast ionization of solid elements and their subsequent homogenization. The derived ionization front velocity compares well with the recent experimental result at LIL laser [5].

ACKNOWLEDGEMENTS

This work was partially supported by EURATOM within the "Keep-in-Touch" activities, the Aquitaine Region Council, and by the European Union's Seventh Framework Programme: the HiPER project # 211737 and the Marie Curie project #230777. Partial support by the Czech Ministry of Education (projects LC528 and MSM6840770022) is acknowledged.

REFERENCES

- [1] J. D. Lindl, P. Amendt, R. L. Berger, S. G. Glendinning *et al.*, Phys. Plasmas **11**, 339 (2004)
- [2] D. H. Kalantar, M. H. Key, L. B. DaSilva, S. G. Glendinning *et al.*, Phys. Rev. Lett. **76**, 3574 (1996)
- [3] M. Dunne, M. Borghesi, A. Iwase, M.W. Jones *et al.*, Phys. Rev. Lett. **75**, 3858 (1995)
- [4] C. Labaune, H. Bandulet, S. Depierreux, K. Lewis *et al.*, Plasma Phys. Control. Fusion **46**, B301 (2004)
- [5] S. Depierreux, C. Labaune, D. T. Michel, C. Stenz *et al.*, Phys. Rev. Lett. **102**, 195005 (2009)
- [6] J. Denavit, and D. W. Phillion, Phys. Plasmas **1**, 1971 (1994)
- [7] R. J. Mason, R. A. Kopp, H. X. Vu, D. C. Wilson *et al.*, Phys. Plasmas **5**, 211 (1998)
- [8] T. Kapin, M. Kucharik, J. Limpouch, and R. Liska, Cz. J. Phys **56**, B869 (2006)
- [9] S. Yu. Gus'kov, and V. B. Rozanov, Quantum Electronics **24**, 696 (1997)
- [10] S. Yu. Gus'kov, J. Russian Laser Research **31**, 574 (2010)